Investigation of Metal-Organic Inhibitor Systems by Local Electrochemical Impedance Spectroscopy (LEIS)
Local electrochemical impedance spectroscopy investigation of corrosion inhibitor films on copper

R. M. Souto[a], J. J. Santana[a,b], A. G. Marques[c] and A. M. Simões[c]

[a] Department of Physical Chemistry, University of La Laguna, E-38200 La Laguna, Tenerife, Canary Islands, Spain
[b] Department of Process Engineering, University of Las Palmas de Gran Canaria, E-35017 Las Palmas de Gran Canaria, Canary Islands, Spain
[c] ICEMS & DEQB, Instituto Superior Técnico, Technical University Lisbon, Avenida Rovisco Pais, 1049-001 Lisboa, Portugal

In this work, the applicability of localized electrochemical impedance spectroscopy (LEIS) to characterize metal-corrosion inhibitor systems has been investigated. Copper corrosion inhibition by benzotriazole (BTA) and 2-mercaptobenzimidazole (MBI) has been studied, and compared to the electrochemical behaviour of the non inhibited metal. A rather wide frequency range of the AC potential signal was employed, namely 50 mHz $\leq f \leq$ 65 kHz. The measurements were conducted for different probe-substrate distances in order to explore the effect of the different component of the localized impedance. Nyquist diagrams exhibit inductive loops in the high frequency range, and capacitive semicircles at intermediate and low frequencies for all the systems investigated, though they were affected in a different extent by the variation of the probe-substrate distance depending on the surface condition of the metal samples, this effect being more notorious for distances smaller than the dimensions of the bi-electrode probe.

Introduction

Most metals undergo spontaneous degradation reactions in the atmosphere if left unprotected. The surface is oxidized and eventually may produce oxide layers or freely dissolve in the environment. The reactions responsible for these processes occur at the interface established between the metal and the medium they are exposed to. Therefore, metals can be protected against corrosion by introducing a barrier film that physically separates the metal from the environment. This is the rationale behind the application of organic layers for the anticorrosion protection of metallic materials, and in particular, the layers formed by inhibitors on metals. 2-mercaptobenzimidazole (MBI) and benzotriazole (BTAH) are probably the most widely employed corrosion inhibitors, their use ranging from copper and its alloys (1-7), to steels (8-11), and to zinc (12-16). They effectively protect these metals in various aggressive environments, and the most accepted mechanism to describe their operation involves the formation of a chemisorbed multilayer of these organic molecules on the surface of the metals. The current understanding of the degradation processes of coated metals exposed to aqueous environments has mainly developed from the information gained

by using conventional electrochemical techniques, including electrochemical impedance spectroscopy (EIS). But EIS data represent an average response for the entire surface, though the results are generally described in terms of localized processes. That is, the observations derived from those measurements may not necessarily represent the real behaviour of the metal/coating interface at the microscopic level.

Since the introduction of scanning microelectrochemical techniques in the corrosion laboratory, which provide *in situ* topographic and electrochemical reactivity information about the surface evolution at the micrometer scale in aqueous environments, several attempts to characterize the organic layers formed on metals have been made. In this field, the greatest success has been found using the scanning vibrating technique (SVET) (17,18). The measurement of localized ionic currents in the electrolyte phase, that are related to the electrochemical activity of either coated or inhibitor-treated surfaces, effectively characterize the reaction sites at the metal-electrolyte interface, as well as the ability of the surface films to protect them (19-22). More recently, the scanning electrochemical microscope (SECM), operated in either feedback or generation-collection modes, is also supplying valuable information concerning the corrosion processes occurring in metals covered by organic coatings (23-24), but it has not been so efficient for the characterization of the films formed by corrosion inhibitors despite a few contributions to the scientific literature (25-28). To overcome the difficulties met by amperometric SECM to characterize metal-inhibitor systems, alternating-current scanning electrochemical microscopy has been employed instead, taking advantage of the fact that this technique does not require a redox mediator in the electrolyte for imaging (29). Furthermore, the impedance response at the tip is sensitive to differences in the local chemical reactivity of the investigated surface (30-32), though the analysis of the resulting impedance spectra remains unclear and it has only been solved for a few model systems until now (33,34).

Actual local measurements of the electrochemical impedance (LEIS) were first conducted by Isaacs et al. (35,36), by measuring the local alternating current density in the proximity of a dual working electrode the electrochemical cell. Various corrosion processes have been investigated using LEIS, namely the progress of delamination in polymer-coated steel (35-37), the contributions of the different phases present in metallic alloys (38,39), and the electrochemical reactivity of inclusions (40) or weld metals (41). In local impedance measurements, the local alternating current density can be obtained using the Ohm's law:

$$i_{loc}(\omega) = \frac{\Delta V_{probe}(\omega) k}{d} \qquad [1]$$

where k is the conductivity of the electrolyte, $\Delta V_{probe}(\omega)$ is the AC potencial difference, and d is the distance between the two sensing wires in the dual working probe. The local impedance is then defined by (42-45):

$$Z_0 = \frac{\tilde{V} - \phi\tilde{}_0}{\tilde{\imath}} \qquad [2]$$

Then, the ohmic impedance is given by:

$$Z_e = \frac{\phi\tilde{}_0 - \phi\tilde{}_\infty}{\tilde{\imath}} \qquad [3]$$

and the impedance Z is obtained through the addition of equations [2] and [3]:

$$Z = Z_0 + Z_e = Z_0 = \frac{\tilde{V} - \tilde{\phi}_\infty}{i_t} \qquad [4]$$

Figure 1 depicts a sketch of these impedance elements for a cylindrical electrode, where $\tilde{V} - \tilde{\phi}_0$ represents the potential difference between the surface of the electrode and a point in the border of the double layer, $\tilde{\phi}_0 - \tilde{\phi}_\infty$ gives the potential difference between that border point and the reference electrode, and $\tilde{V} - \tilde{\phi}_\infty$ for the potential difference between the electrode surface and the reference electrode located in the bulk of the electrolyte. In this way, the local ohmic impedance is found to vary with the radial position.

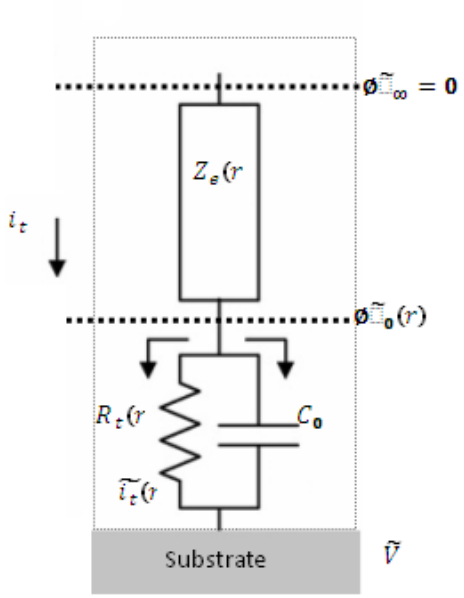

Figure 1: Sketch of the impedance components found in a disk electrode (42-44). Z_e is the local ohmic impedance, C_0 is the interfacial capacitance, and R_t is the charge transfer resistance. (r represents a variable that depends on the radial position.

Regarding the distance comprised between the local probe and the substrate on the LEIS response, it has been proposed (46) that it plays a role on the local ohmic impedance which is the origin of changes in the inductive loop occurring in Nyquist diagrams when the probe is located in close proximity to the investigated surface.

In this contribution we have employed LEIS to investigate various metal-corrosion inhibitor systems, with special attention to the effect of variations in the probe-substrate distance.

Experimental

Measurements were performed on 99.99% copper purity plates (Goodfellow, UK) of dimensions 3 cm x 3 cm and 1 mm of thickness. The surface of the samples was ground mechanically using a sequence of emery papers, namely 800, 1200 and 4000 grit, and then polished with 0.3 μm alumina slurries, degreased with acetone, rinsed with bi-distilled water and dried to air. Benzotriazole (BTAH; Avocado Research Chemicals Ltd., UK) and 2-mercaptobenzimidazole (MBI; Aldrich, UK) were used as received. All aqueous solutions

were prepared using Milli-Q water. Measurements were performed in naturally aerated solutions at ambient conditions (22ºC). For the preparation of the inhibitive films on the copper samples, the metal plates were immersed either in 0.1 M NaCl + 1 mM MBI or in 0.1 M NaCl + 1 mM BTA aqueous solutions for 1 hour. The test electrolyte employed in the LEIS measurements was 1 mM NaCl.

Localised electrochemical impedance spectroscopy (LEIS) was carried out with a LEIS340 (Uniscan, UK) connected to a 1286 electrochemical interface (Solartron, UK) and a 1250 frequency response analyzer (Solartron, UK). This method used a five-electrode configuration. LEIS measurements were taken from the ratio of the applied AC voltage to the local AC current density. The applied voltage ($\Delta V_{applied}$) was the potential difference between the working electrode and the reference electrode, and the frequency range was 50 mHz $\leq f \leq$ 65 kHz. The local AC current density (i_{local}) was calculated using equation [1]. The local impedance Z_{local} is calculated by the relationship

$$Z_{local} = \frac{\Delta V_{applied}}{i_{local}} \qquad [5]$$

Results and discussion

Figura 2 shows the Nyquist diagrams of the localized impedance responses for the bare copper sample immersed in 1 mM NaCl with different probe-substrate distances. A capacitive semicircle is observed in the low frequency range, which does not significantly change in shape as distance is changed. Additionally, an inductive loop occurs in the high frequency range, which is related to the localized ohmic impedance (42-44,47).

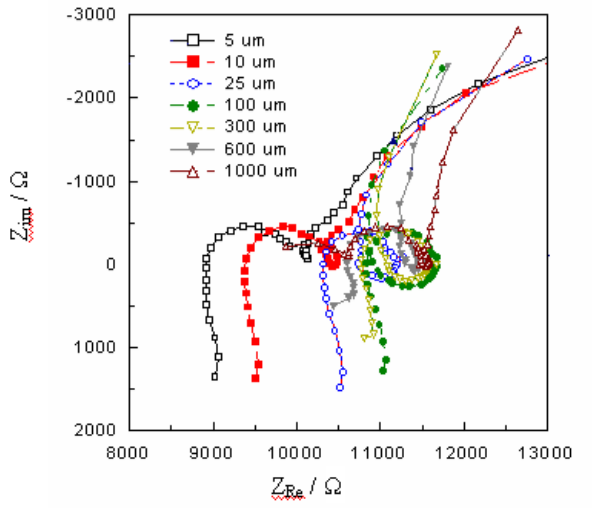

Figure 2: Nyquist diagrams of the high frequency inductive loop occurring in the localized impedance responses for the bare copper sample immersed in 1 mM NaCl with different probe-substrate distances as indicated in the plot.

The potential distribution on the metal surface is uniform and the radial component of the current density is zero, whereas the normal component of the current density is non uniform (47). A similar inductive loop was obtained by Blanc et al. (47), though in our case the centre of this loop shifts to higher impedance values with the increase of the probe-substrate distance for d < 25 μm. In addition to the shift towards bigger impedance values, it is also observed

that the size of the loop also varies with the probe-substrate distance. In both cases, the ohmic impedance is given by a complex quantity, and it is independent of the radial position, but it depends on the probe-substrate distance for distances close to the dimensions of the probe. On the other hand, the capacitive semicircle occurring in the low and intermediate frequency range, is related to the corrosion resistance of the metal. The size of the semicircle grows as the probe-substrate distance is increased, this effect being more notorious for $d > 25$ μm.

In the case of the copper samples treated with the inhibitors, the localized impedance diagrams also contain inductive loops in the high frequency range. Figures 3 and 4 depict the Nyquist diagrams for the high frequency range of the LEIS measurements performed at different probe-substrate distances on the samples protected with an inhibitor-containing layer of BTA and MBI, respectively.

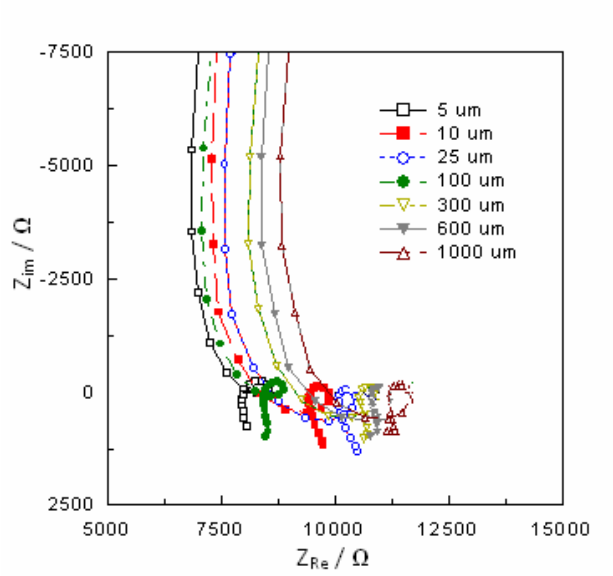

Figure 3: Nyquist diagrams of the high frequency inductive loop occurring in the localized impedance responses for the BTA-treated copper sample immersed in 1 mM NaCl with different probe-substrate distances as indicated in the plot.

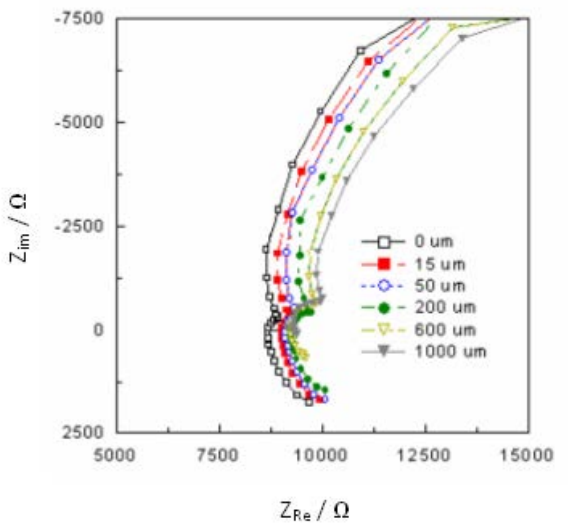

Figure 4: Nyquist diagrams of the high frequency inductive loop occurring in the localized impedance responses for the MBI-treated copper sample immersed in 1 mM NaCl with different probe-substrate distances as indicated in the plot.

Yet some differences can be observed for the two inhibitor-treated systems already in the high frequency range of the diagrams. Whereas the inductive loop for the copper sample treated with BTA exhibited the same trend with the probe-substrate distance described before for the untreated copper sample, an apparently distance-independent behaviour is shown by the sample treated with MBI, thus presenting a specific distribution of the current components compared to the other two systems. Conversely, MBI does not present a specific effect for the capacitive semicircle occurring in the low and intermediate frequency ranges.

More information can be extracted from the direct comparison of the Nyquist diagrams of the localized impedances measured for the bare and the inhibitor-modified copper samples the three tested systems. Figure 5 gives the plots for two probe-substrate distances which are just below and above the dimensions of the probe. In this way, an increase in the diameter of the capacitive semicircle in the sequence Cu < Cu-MBI < Cu-BTA is observed.

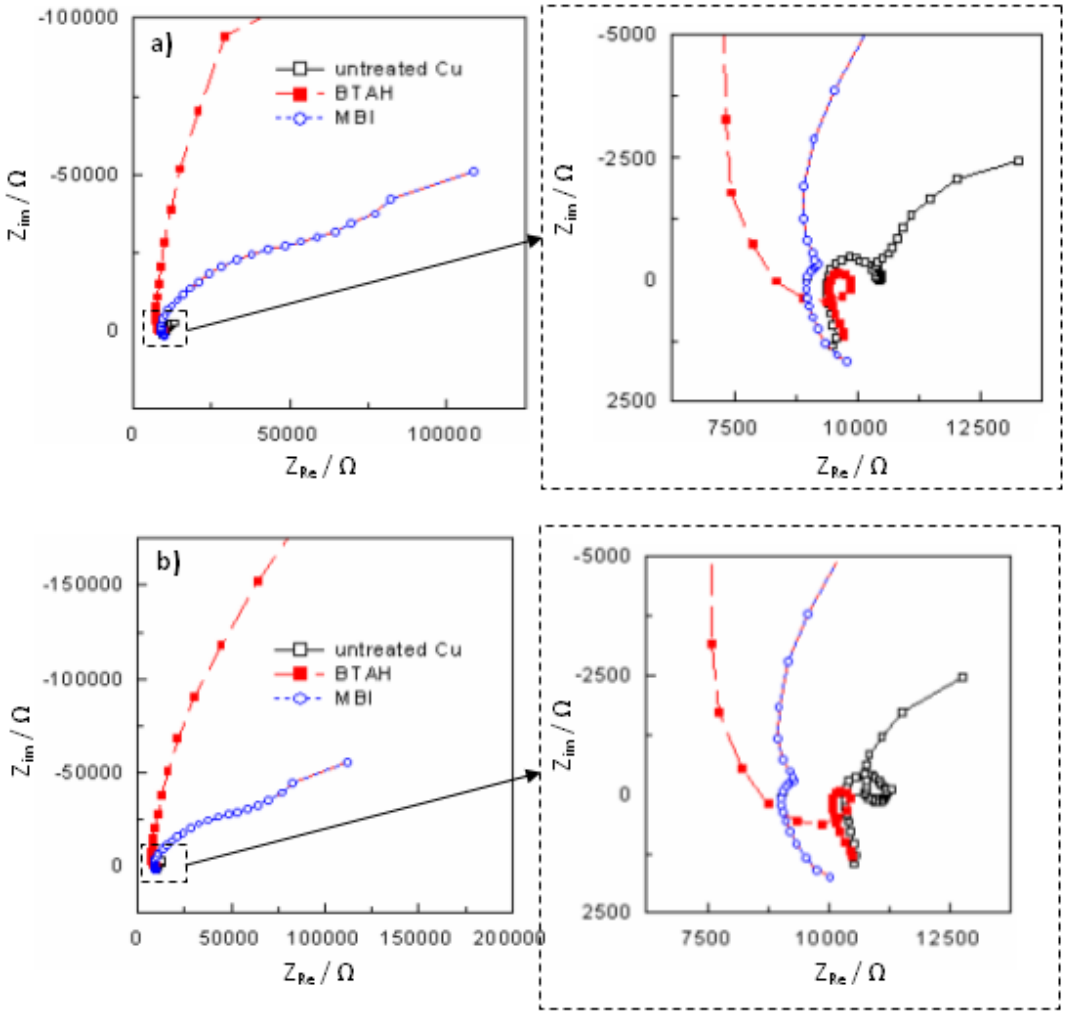

Figure 5: Nyquist diagrams of the localized impedance responses for copper samples with different pretreatments as indicated in the plots. The LEIS were measured during the immersion of the samples in 1 mM NaCl. Probe-substrate distances: (a) 10, and (b) 25 µm.

The different corrosion resistance of the surface films formed on the copper samples is more clearly observed from the inspection of the Bode diagrams given in Figure 6. In this way, the highest resistance is provided by the BTA-treated simple, which delivers resistance values one order of magnitude greater than MBI. This result contradicts previous observations on the Cu-BTA and Cu-MBI systems derived from EIS measurements (48), and from the

combined use of SECM and SVET (27,49). In those studies, MBI exhibited the best corrosion resistance properties, and they were observed even for rather short durations of the treatment. Nevertheless, the differences in the inductive loops occurring in the high frequency range, may account for the reported discrepancy. Indeed, the centres of the inductive loops shift to greater impedance with the increase of the probe-substrate distance for the untreated and the BTA-treated copper samples (cf. Figures 2 and 3), whereas they remain in the same position in the case of the simple treated with MBI. That is, MBI is the compound that produces the greater modification of the localized ohmic impedance from that corresponding to the bare metal, as to become practically negligible independent of the probe-substrate distance.

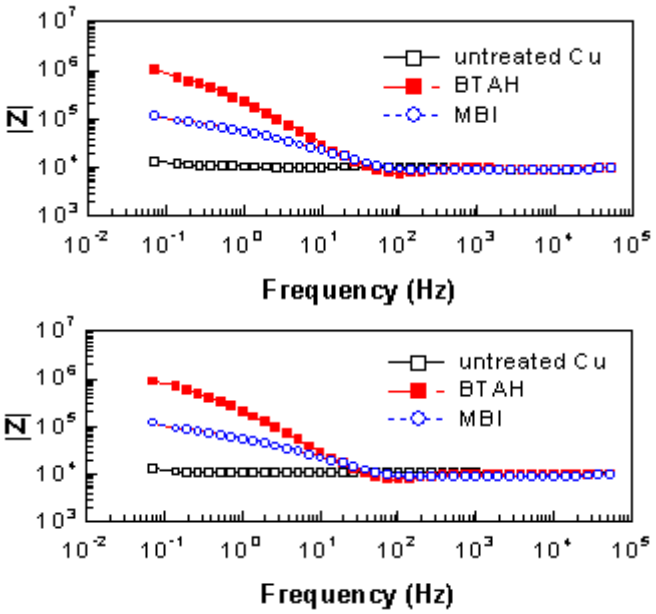

Figure 6: Nyquist diagrams of the localized impedance responses for copper samples with different pretreatments as indicated in the plots. The LEIS were measured during the immersion of the samples in 1 mM NaCl. Probe-substrate distances: (a) 10, and (b) 25 μm.

Conclusions

Localized electrochemical impedance spectroscopy (LEIS) supplies quantitative information regarding the protection characteristics of corrosion inhibitors applied on copper. The shape of the Nyquist diagrams varies with changes in the distance between the probe and the substrate for distance in excess of the probe dimensions. A capacitive semicircle is measured in the low and intermediate frequency ranges for the bare metal as well as for the samples treated with BTA and MBI, whereas inductive behaviours occur in the high frequency range of the spectra. The formation of a MBI-containing surface film on copper affects the localized ohmic resistance that shows and inductive behaviour independent of the probe-substrate distance, conversely to the behaviours observed for the untreated copper and for the sample treated with BTA.

References

1. G. W. Poling, *Corros. Sci.*, **10**, 359 (1970).
2. S. Thibault and J. Talbot, *Met. Corros-Ind.*, **50**, 51 (1975).

3. T. Notoya and G. W. Poling, *Corrosion*, **32**, 216 (1976).
4. F. Mansfeld, T. Smith and P. Parry, *Corrosion*, **27**, 289 (1971).
5. D. Chadwick and T. Hashemi, *Corros. Sci*., **18**, 81 (1978).
6. D. Tromans and R. Sun, *J. Electrochem. Soc.*, **138**, 3235 (1991).
7. G. Xue, X.- Y. Huang, J. Dong and J. Zhang, *J. Electroanal. Chem.*, **310**, 139 (1991).
8. M. Th. Makhhuf, S.A. El-Shatory and A. El-Said, *Mater. Chem. Phys.*, **43**, 76 (1996).
9. A. N. Starchak, A. N. Krasovskii, V. A. Anishchenko, L. D. Kosnkhina, *Zashch. Met.*, **30** (4), 405 (1994).
10. G. L Makovei., V.G. Ushakov, V. K. Bagin, V. P. Shemshei, *Zashch. Met.*, **22** (3), 470 (1986).
11. L. Wang, *Corros. Sci.*, **43**, 2281 (2001).
12. L. Wang, J.-X. Pu, H.-Ch. Luo, *Corros. Sci.*, **45**, 677 (2003).
13. M. S. Abdel Aal, A. El-Saied, *Trans. SAEST*, **16**, 197 (1981).
14. M. Troquet, J.P. Labbe, J. Pagetti, *Corros. Sci.*, **21**, 101 (1981).
15. C. F. Yang, Y. X. Bai, *Appl. Chem.*, **12** (6), 56 (1995).
16. B. M. Abo El-Khair, S.M. Abdel-Wahaab, M. M. El-Sayed, *Surf. Coat. Technol.*, **27**, 317 (1986).
17. R. S. Lillard, in *Analytical Methods in Corrosion Science and Engineering*, P. Marcus and F. Mansfeld, Editors, p. 571, CRC Press, Boca Raton (FL) (2006)
18. S. Lamaka, R. M. Souto and M. G. S. Ferreira, in *Microscopy: Science, Technology, Applications and Education, Vol. 4,* A. Méndez-Vilas, J. Díaz, Editors, p. 1769, Formatex, Badajoz (2010).
19. A. C. Bastos, M. L. Zheludkevich and M.G. S. Ferreira, *Prog. Org. Coat*., **63**, 282 (2008).
20. O. V. Karavai, A. C. Bastos, M. L. Zheludkevich, M. G. Taryba, S. V. Lamaka and M. G. S. Ferreira, *Electrochim. Acta*, **55**, 5401 (2010).
21. D. Borisova, H. Möhwald and D. G. Shchukin, *ACS Nano*, **5**, 1939 (2011).
22. S. J. García, H. R. Fischer, P. A. White, J. Mardel, Y. González-García, J. M. C. Mol and A. E. Hughes, *Prog. Org. Coat.*, **70**, 142 (2011).
23. L. Niu, Y. Yin, W. Guo, M. Lu, R. Qin and S. Chen, *J. Mater. Sci.*, **44**, 4511 (2009).
24. Y. González-García, J. J. Santana, J. González-Guzmán, J. Izquierdo, S. González and R. M. Souto, *Prog. Org. Coat.*, **69**, 110 (2010).
25. K. Mansikkamäki, P. Ahonen, G. Fabricius, L. Murtomäki and K. Kontturi, *J. Electrochem. Soc.*, **152**, B12 (2005).
26. K. Mansikkamäki and C. Johans, K. Kontturi, *J. Electrochem. Soc.*, **153**, B311 (2006).
27. J. Izquierdo, J. J. Santana, S. González and R.M. Souto, *Electrochim. Acta*, **55**, 8791 (2010).
28. J. Izquierdo, L. Nagy, J. J. Santana, G. Nagy and R.M. Souto, *Electrochim. Acta*, **58**, 707 (2011).
29. M. Pähler, J. J. Santana, W. Schuhmann and R. M. Souto, *Chem. Eur. J.*, **17**, 905 (2011).
30. A.S. Baranski and P.M. Diakowski, *J. Solid State Electrochem.*, **8**, 683 (2004).
31. K. Eckhard, T. Erichsen, M. Stratmann, W. Schuhmann, *Chem. Eur. J.*, **14**, 3968 (2008).
32. K. Eckhard and W. Schuhmann, *Analyst*, **133**, 1486 (2008).
33. D. Trinh, M. Keddam, X. R. Novoa and V. Vivier, *Chem. Phys. Chem*., **12**, 2169 (2011).
34. D. Trinh, M. Keddam, X. R. Novoa and V. Vivier, *Chem. Phys. Chem*., **12**, 2177 (2011).

35. L. V. S. Philippe, G. W. Walter and S. B. Lyon, *J. Electrochem. Soc.,* **150**, B111 (2003).
36. J. B. Jorcin, E. Aragon, C. Merlatti and N. Pebere, *Corros. Sci.*, **48**, 1779 (2006).
37. G. Baril, C. Blanc, M. Keddam and N. Pebere, *J. Electrochem. Soc.,* **150**, B488 (2003).
38. G. Galicia, N. Pebere, B. Tribollet and V. Vivier, *Corros. Sci.*, **51**, 1789 (2009).
39. H. Krawiec, V. Vignal and J. Banas, *Electrochim. Acta*, **54**, 6070 (2009).
40. T.Y. Jin and Y.F. Cheng, *Corros. Sci*., **53**, 850 (2011).
41. G. A. Zhang and Y. F. Cheng, *Corros. Sci*., **51**, 1714 (2009).
42. V. M.- W. Huang, V. Vivier, M. E. Orazem, N. Pébère and B. Tribollet, *J. Electrochem. Soc.,* **154**, C81 (2007).
43. V. M.- W. Huang, V. Vivier, I. Frateur, M. E. Orazem and B. Tribollet, *J. Electrochem. Soc.,* **154**, C89 (2007).
44. V. M.- W. Huang, V. Vivier, M. E. Orazem, N. Pébère and B. Tribollet, *J. Electrochem. Soc.*, **154**, C99 (2007)
45. V. M.- W. Huang, S.- L. Wu, M. E. Orazem, N. Pébère, B. Tribollet and V. Vivier, *Electrochim. Acta*, **56**, 8048 (2011).
46. I. Frateur, V. M. Huang, M. E. Orazem, B. Tribollet and V. Vivier, *J. Electrochem. Soc.,* **154**, C719 (2007).
47. C. Blanc, M. E. Orazem, N. Pébère, B. Tribollet, V. Vivier and S. Wu, *Electrochim. Acta,* **55**, 6313 (2010).
48. D.- Q. Zhang, L.- X.Gao, G.- D. Zhou, *Corros. Sci.,* **46**, 3031 (2004).
49. J. Izquierdo, J.J. Santana, S. González, R.M. Souto, *Prog. Org. Coat.*, submitted.